Angle-resolved energy distribution of re-emitted positrons from a W(100) single crystal

K. Sudarshan,[1] S. N. Samarin,[1] P. Guagliardo,[1] V. N. Petrov,[1,2] A. H. Weiss,[3] and J. F. Williams[1]

[1]*ARC Centre of Excellence for Antimatter and Matter Studies, School of Physics, The University of Western Australia, Crawley, Perth, Western Australia 6009, Australia*

[2]*St. Petersburg State Polytechnical University, Polytechnicheskaya 29, St. Petersburg 195251, Russia*

[3]*Physics Department, University of Texas at Arlington, Arlington, Texas 76019-0059, USA*

(Received 16 November 2012; published 13 February 2013)

Angular distribution of backward re-emitted positrons from a W(100) single crystal have been measured for incident positron energies of 250 and 600 eV. The width of the angular distribution was broader than that predicted by a model of re-emission that assumes complete thermalization of positrons in the solid. Angle-resolved energy distribution of re-emitted positrons showed that the mean energy of the emitted positrons increased with angular deviation from normal. The increase is explained in terms of energy-dependent refraction of positrons traversing the potential step at the surface. The results are in qualitative agreement with a one-dimensional step model of positron re-emission. The observed angular distribution and energy distributions qualitatively matched calculated data if a sample effective temperature of four times the actual temperature is assumed. This suggests the emission of incompletely thermalized positrons at low energy of incident positrons.

DOI: 10.1103/PhysRevB.87.085418 PACS number(s): 79.20.Mb, 41.75.Fr, 68.35.−p, 42.25.Gy

I. INTRODUCTION

The influence of electrostatic dipole at the surface is opposite for the positron in comparison with the electron. This fact, coupled with electrostatic interactions of positrons with electrons and ion cores inside the solid, makes the positron work function negative for many metals. As a result, implanted and thermalized positrons which manage to diffuse back to the surface can be re-emitted with kinetic energy equivalent to the positron work function (ϕ^+) of the material.[1] This phenomenon is referred to as "positron re-emission."

The materials for moderation of energetic positrons to low energies are based on this process. With the advent of new experimental techniques that use energy-tunable positron beams, the demand for high intensity and focused positron beams is increasing.[2,3] The intensity, focusing, and brightness of the beam depend on the inherent re-emission characteristics of the moderator. The optimization of beam transport and focusing methods also depends on the inherent spread in the angular and energy distribution of the re-emitted positrons.

Tungsten is the most widely used moderator in the positron beams worldwide. Wide usage of the tungsten as moderator is due to its high positron re-emission yield.[4] The conditioning methods of a W moderator involving high-temperature annealing and surface cleaning are optimized and are followed by most users of the positron beams.[5–7] However, there is still a large scope and efforts are continuously on for improving the intensity, brightness, and polarization of the beam. To further decrease the energy spread and beam diameter, remoderation steps are also used.[8] Hence, it is necessary to understand quantitatively all the measurable quantities in the re-emission process and at different incident energies, both to enhance the positron beam characteristics and to fundamental understanding of positron solid interactions.

In the one-dimensinal (1D) step model of re-emission process, the implanted positrons are assumed to completely thermalize in the bulk and a fraction of them manage to diffuse to the surface before annihilation. These thermal positrons gain kinetic energy equivalent to the work function during the re-emission process where positrons transverse a 1D potential step.[9] This theory also provides an explanation of the angular and energy distributions of electrons emitted from the surfaces with negative electron affinity.[10] The refraction of positrons at the surface while traversing the potential step focusses the re-emitted positrons towards the surface normal. The extent of focusing depends on the initial kinetic energy and the height of the potential step.

The energy distribution of positrons inside the solid is determined by thermalization processes. At low temperatures, the re-emitted positron energy distribution from Ni(100) in the direction normal to the surface was reported to be broader than kT_{samp}, where T_{samp} is the actual temperature of the sample in K and k is the Boltzmann constant. Agreement with theory could only be achieved by assuming an effective sample temperature of 4–5T_{samp} due to incomplete thermalization of positrons before re-emission.[11,12] However, it may be noted that most of the measurements on energy and angular distribution of re-emitted positrons are carried out at high incident positron energies of the order of few keV, where the implantation depths are large and the re-emission process is diffusion controlled.[11–13] At low incident energies, where the implantation depths are comparable to or lower than the diffusion length of the thermal positron, assumption of complete thermalization before re-emission may be invalid.

While traversing the 1D step potential, the positrons with lower kinetic energy (inside the solid) are refracted more towards the surface normal than the positrons of higher energy. These differences in the refraction with initial kinetic energy appear as an increase in the low-energy cutoff at non-normal angles in the Γ-point electron emission from negative electron affinity surfaces.[14] However, similar effects have never been reported in positron emission. Angle-resolved positron energy distributions from Cu, W, and Al surfaces have been measured.[11–13] The energy distributions became broader and the peak energy decreased as $\cos^2\theta$ with an increase in the angular deviation from normal to the surface, "θ." In these studies, the "projection of positron energies" along the normal

to the surface was measured rather than the total energy as a negative bias was applied to the sample to retard the re-emitted positrons.

In the present study, the angular distribution of the backward re-emitted positrons and the angle-resolved energy distributions are measured. The results are discussed in terms of a 1D step model of positron re-emission. The results provide a better understanding of re-emission processes at low positron incident energies and are very important for optimizing the remoderation conditions where the primary aim is to decrease the angular and energy spread of the re-emitted positrons.

II. EXPERIMENT

Re-emission measurements were performed using the electrostatic slow positron beam at The University of Western Australia. The design of the beam is described in Ref. 15. The energy of the incident positrons was determined by the accelerating voltage of the moderator. Positrons were electrostatically transported to the experimental chamber which was held at a vacuum of 10^{-10} mbar. The incident beam intensity was $\sim 700 e^+$/sec, and the diameter of the beam spot was ~3–4 mm. The W(100) crystal was in the center of the chamber on a manipulator (x, y, z, θ). A position sensitive microchannel plate (MCP) detector, with a combination of retarding grids in front, was at a fixed position of 45° with respect to the incident beam. The MCP had a 40-mm active diameter and the sample to detector distance was 100 mm. The wide acceptance angle of the detector ($\sim \pm 11°$) was necessary to achieve reasonable count rates.

Prior to measurements, the W(100) single crystal was cleaned following the standard procedures reported.[16–18] The crystal was heated to about ~1400 °C in the presence of 10^{-8} mbar oxygen for 3 min, followed by high-temperature annealing at ~2400 °C using electron bombardment and allowing the sample to cool for 2 h. The cleaning procedure was repeated at regular intervals. The MCP in combination with the retarding grids was used as retarding field analyzer (RFA), to measure the energy of the re-emitted positrons (Fig. 1). Input of the MCP was biased to −200 V with respect to ground. This potential accelerates positrons passing grid 2 enabling their better detection, and also aids in rejection/reduction of the secondary electron detection. The W(100) crystal was very thick (~1 mm) and the positrons were measured only in backward hemisphere (no transmission).

The angular distributions of the positrons were measured by rotating the sample in 2° increments to change the detection angle of the re-emitted positrons. The count rates of positrons under the work function peak were plotted to determine the angular distribution.

Energy measurements were carried out at selective angles for longer times. Initially the sample was parallel to MCP and incident beam is at 45°. In this geometry, the positrons emitted in the direction normal to the sample (with in the acceptance angle) are measured. When the angle of the sample was rotated by θ, the positrons emitted with an angular deviation of θ with respect to the normal to the crystal surface were detected. The arrangements and potentials of the retarding grid in our system were such that the re-emitted positrons enter a field-free region. As seen from Fig. 1, at any orientation of the sample, the measured positrons are in the direction normal to the retarding grid and the total energy of positrons is measured ($E \sim E_z$).

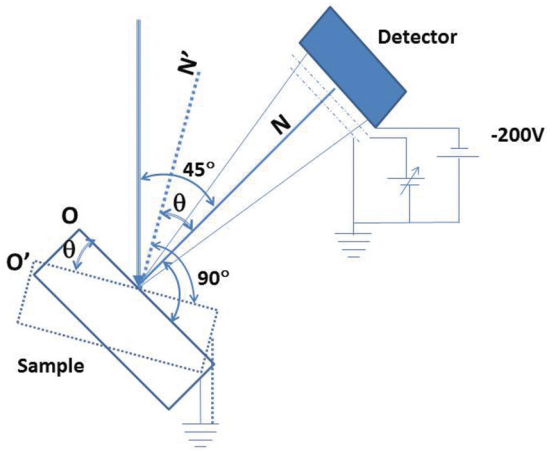

FIG. 1. (Color online) A schematic of the experimental arrangement for measuring re-emitted positron energy and angular distributions. The orientation of the sample (O') with N' as its surface normal shown with dotted lines is obtained by rotating the sample by θ from the initial orientation (O with N as normal).

III. RESULTS AND DISCUSSION

The retarding curve of re-emitted positrons was initially measured with the sample parallel to the detector. The measured retarding curve and the negative of its derivative, which gives the energy distribution of detected positrons, are given in Fig. 2. Although the normal to the crystal surface is also the normal to the detector in this geometry, the wider acceptance angles of the detector allows for the inclusion of positrons which are at an angle with the normal to the retarding grid. For these positrons, the "projection of energy" in the direction normal to the grid is measured. The angle of measurement in further discussion refers to the angle between the normal to the surface and the normal to the detector/grid.

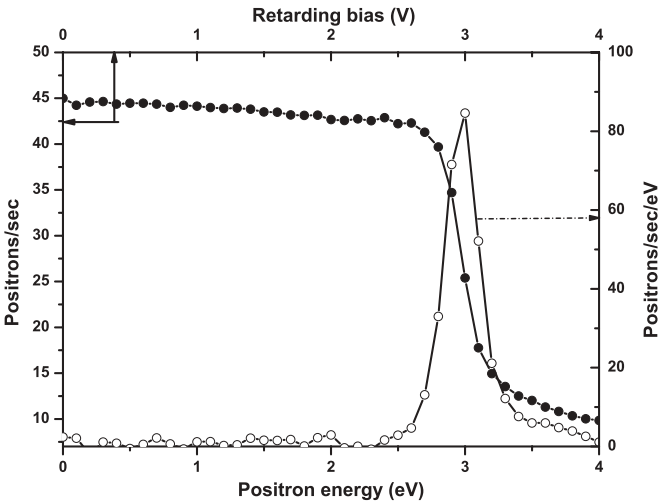

FIG. 2. Positron counts with retarding bias on grid (filled circles) and negative of its derivative showing the energy spectrum (open circles) at incident positron energy of 600 eV.

The centroid of the energy spectrum was found to be 2.93 ± 0.01 eV. The work function of W(100) is reported as −1.9 ± 0.3 eV in 10^{-6} Torr pressure by Jin *et al.*,[19] −2.48 ± 0.05 eV by Amarendra *et al.*,[5] and −3.0 ± 0.3 eV by Chen *et al.*[13] Hugenschmidt *et al.*[20] reported the work function to be −2.5 ± 0.2 eV for unannealed and −3.00 ± 0.15 eV for the well-annealed sample. The large scatter in the values indicates the sensitivity of the work function to surface conditions and difficulty in correction methods for the contact potential differences between the sample and detection system. The peak position in Fig. 2 is close to that reported by Chen *et al.*[13] and Hugenschmidt *et al.*,[20] and will be used as the work function in further discussion.

A. Angular distribution

For the measurement of the angular distribution the positron retarding curve was recorded at each angle with retarding bias steps of 1 V from 0 to 6 V, and positrons in the energy range 1–5 eV were counted as re-emitted positrons. This is a reasonable assumption based on the energy distribution shown in Fig. 2. The count rates of these positrons as a function of angle between the normal to the sample and the detector axis are shown in Fig. 3 for incident energies of 250 and 600 eV. The count rates are normalized to unity in the direction normal to the surface (0°). It is clearly seen from Fig. 3 that the angular distribution is independent of the incident energy for the two energies used. The measured data are transposed with respect to the normal to the crystal surface as the angular distribution is expected to be symmetric with respect to the normal and is shown in Fig. 3 as open symbols. The transposed and directly measured data are in good agreement in the angular range of ∼± 15° with respect to the normal. The measured count rates in the angular range of < − 15° are higher than transposed, i.e., the count rates show tailing in negative angular deviation with respect to normal.

As discussed in the experimental section, the emission angle of detected positrons was changed by rotating the sample, which also simultaneously changed the angle of incidence. In the convention used to denote the angles in Fig. 3, a negative angle refers to the situation where incident beam and detected positrons are on opposite sides of the normal to the surface while a positive angle refers to the situation where the incident beam and detected positrons are both in the same quadrant with respect to the normal to the surface. Hence, the tailing in the angular distribution curve at negative angles with respect to the surface normal might be due to contributions from forward scattered positrons which may not be truly re-emitted positrons. Ignoring the tailing at negative angles, the angular distribution was fitted with a Gaussian function and the full width at half maximum (FWHM) was found to be 24.5 ± 0.5°. The angular distribution of re-emitted positrons from a W(100) film of 1000 Å thickness at an incident energy of 5 keV was reported by Chen *et al.*[13] and is also given in Fig. 3. The angular distribution in the present measurements is narrower than that reported by Chen *et al.* (FWHM ∼30°) but broader than reported by Fisher *et al.*[8] on W(110) + C which has a positron work function in a similar range, and for an incident energy of 3 keV.

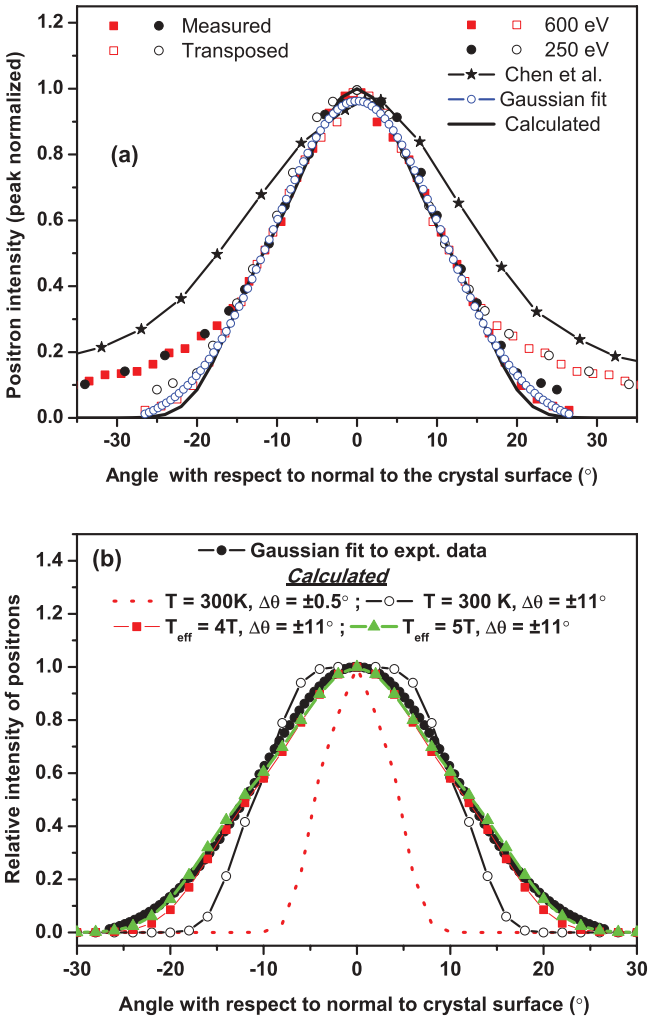

FIG. 3. (Color online) (a) Angular distribution of backward re-emitted positrons from W(100) at an incident energy of 250 (circle) and 600 eV (square) and forward re-emitted positrons from 1000-Å W(100) film with 5 keV incidence energy from Chen *et al.* (Ref. 13). The open symbols correspond to transposed data with respect to normal to the crystal surface. Caclulated data is with $T_{\text{eff}} = 4T_{\text{samp}}$ [see legend of (b) for details]. (b) Calculated angular distributions with various parameters (effective temperature and acceptance angle) in terms of 1D step model of positron re-emission. The $\phi^+ = -2.93$ eV and $(m^*/m) = 1$. Gaussian fit to the experimental angular distribution is also shown in the figure as filled circles.

The angular distribution of re-emitted positrons can be calculated to a first approximation by assuming that the incident positrons are thermalized in the solid and that during re-emission, the work function (ϕ^+) of the material provides a one-dimensional potential step at the surface. This provides an additional kinetic energy of $-\phi^+$ eV in the direction normal to the crystal surface. Equating the components of the momentum of positron inside and outside solid in the direction parallel to surface of the crystal, the final angle of emission (θ) with respect to the normal to the crystal is related to the initial angle in the solid (θ') by

$$\sin\theta = \left[\left(\frac{m^*}{m}\right)\left(\frac{E_s}{E_s - \phi^+}\right)\right]^{1/2} \sin\theta' \qquad (1)$$

where (m^*/m) is the effective mass ratio and E_s is the kinetic energy of the positron inside the solid. Assuming that the incident positrons are completely thermalized (sample temperature $T_{\text{samp}} = 300$ K), the effective mass ratio of ~ 1, $\phi^+ = -2.93$ eV, and the initial direction of thermalized positrons inside solid is isotropic, the expected angular distribution is calculated and is shown in Fig. 3(b). The calculated angular distribution is much narrower than the experimentally observed angular distribution even after accounting for the angular acceptance of the detector. The shape of the angular distribution curve at $T_{\text{samp}} = 300$ K and acceptance angle of $\pm 11^\circ$ is clearly seen to differ significantly from the experimental data.

From Eq. (1), the angular distribution would be broader by assuming a higher effective mass ratio but the reported[21] m^*/m of up to 1.5 was not sufficient to reproduce the experimental data. The current angular distribution can be reproduced by using an effective temperature (T_{eff}) of the sample as $4T_{\text{samp}}$. The calculated angular distribution with $T_{\text{eff}} \sim 4T_{\text{samp}}$ (1200 K) is found to be in reasonable agreement with the experimental data as seen in Fig. 3(b). It has been demonstrated that the positron angular distribution at low sample temperatures is broader than expected from thermal broadening alone, due to incomplete thermalization (thermalization times are longer at low temperatures) while it is consistent at higher temperatures.[11] In the present case, the energy of the incident positrons is relatively low. The mean implantation depth of the positrons in tungsten assuming a Makhovian implantation profile[4] is less than 1 nm while the thermal positron diffusion length is greater than 50 nm. The very small implantation depth compared to thermal diffusion length makes emission of positrons that are incompletely thermalized in the solid very likely and the assumption of higher T_{eff} very reasonable. With the large angle of acceptance involved in our measurements, it can be safely concluded that the angular distribution at these incident energies is consistent with $T_{\text{eff}} \sim 4$–$5T_{\text{samp}}$.

B. Energy distribution

Positron retarding measurements were also carried out in finer voltage steps at select angles. The retarding curves were then smoothened by adjacent averaging and the smoothened data were differentiated to obtain the energy distributions. Typical positron retarding curves and energy distributions at various angles with respect to the normal to the surface of the sample and at an incident energy of 250 eV are shown in Fig. 4. It is clearly seen that the energy distributions of positrons emitted in off-normal angles have higher mean. The angle dependent energy spectra were also measured for 600 eV incident positrons. The energy spectra were fitted with Gaussian profile and the deviation of the centroid from that measured in the normal direction is plotted in Fig. 5. The increase in the centroid was similar for deviation from normal in either direction and at both incident energies used in the study.

Since the refraction of the positron trajectories at the surface of the crystal is energy dependent, positrons of higher energy inside the solid are refracted towards the normal to the crystal surface to a lesser extent. Hence we expect a shift in the energy distribution to higher energies at larger angles with respect to the normal to the crystal surface. In earlier measurements of the angle-resolved positron re-emission energy, the E_z component of the energy spectrum was measured rather than the actual energy.[11–13] Hence, the peak position in the energy curve shifted to lower energies at off-normal angles as $\cos^2\theta$ and the effects of refraction could not be observed.

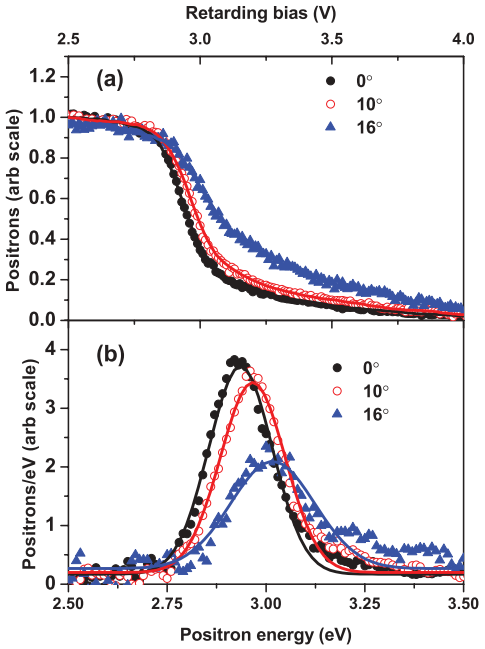

FIG. 4. (Color online) (a) Retarding curves of positron emitted at various angles with respect to the normal to the surface. Total numbers of positrons are normalized. (b) The energy distribution of positrons emitted at different angles. The lines are Gaussian fit to the data.

In our measurements, the subtle effects of positron refraction at the surface could be observed as the energy spectrum was measured by creating a field-free region between the sample and the detector as described in Fig. 1. The positrons are retarded at the grid in front of the detector and the positrons

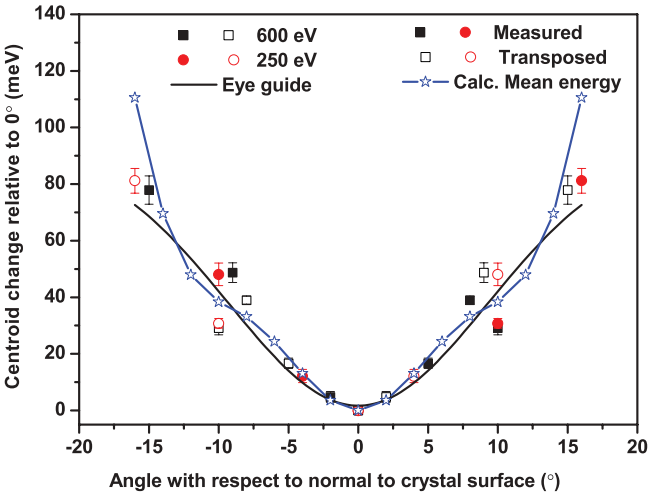

FIG. 5. (Color online) Change in mean energy of the re-emitted positrons with emission angle with respect to the normal to the surface.

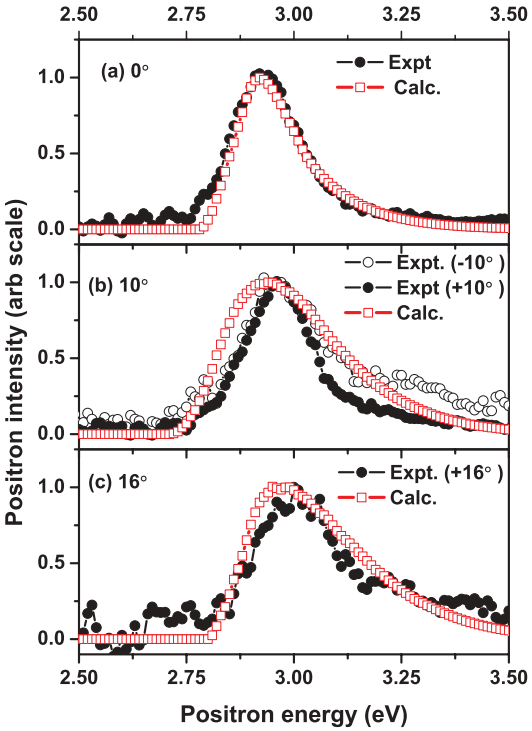

FIG. 6. (Color online) Experimental and calculated energy spectra of re-emitted positrons at various angles. The calculated data are ten-point smoothened by adjacent averaging to match the experimental procedures adopted in measuring the energy spectra.

pass the grid in the direction normal to it ($E_z \sim E$). However, due to the wider acceptance angle involved, the positrons that are not incident in the direction normal to grid, whose $E_z < E$, also get included in the measurements. Due to this, the observed increase in energy could be lower than expected based on refraction of positrons at the surface.

To calculate the differences expected in the spectrum shape with angle, the energy spectra at different angles was calculated using the 1D step model described above. In these calculations, the positrons in the solid are taken to be thermalized and emission direction was random. Taking the energy distribution to be Maxwellian (in steps of 0.01 eV) and the initial direction to be varying between -90 and 90°, the expected angle of emission and the energy spectra at various detection angles were calculated. Angular acceptance of the detector was accounted for in the calculations by taking the "projection of energy" on to the normal to the grid at any measurement angle rather than the actual energy. The calculated energy spectra at each angle (with an energy spacing of 0.01 eV, the same as the steps of retarding curve) was smoothened by ten-point adjacent averaging to match procedures adopted in obtaining the experimental energy spectra. The mean of the calculated energy spectra was also determined.

The calculated spectra and the mean energy deviation angle with respect to the surface normal were in qualitative agreement when an effective temperature of 1200 K ($4T_{\text{samp}}$) was assumed. The calculated energy spectra were much narrower than the measured spectra if the equilibrium temperature of the positrons in the solid was taken as 300 K. Better agreement could be obtained by assuming the acceptance angle of our detection system in the range 9–10° instead of geometrically calculated 11°. A similar match in the mean energy deviations could also be obtained by increasing the effective temperature to about $4.5T_{\text{samp}}$–$5T_{\text{samp}}$. The accuracy of our measurements is not sufficient enough to point to the exact temperature to be used and it was seen even in angular distributions that effective temperature of the 4–$5T_{\text{samp}}$ range explains the observed data. The calculated mean energy deviation with acceptance angle of $\pm 9.5°$ and effective temperature of $4T_{\text{samp}}$ is given in Fig. 5 and the calculations match the observed trends in the measured data. The energy spectra at typical angles (0°, 10°, and 16°) with respect to the normal are given in Fig. 6. The peak maxima in all the spectra (Fig. 6) are normalized to unity. Closest agreement in the energy spectra (at 0°) could be obtained by shifting the calculated spectra to lower energy by ∼0.1 eV or by calculating the spectrum using a work function lower than the peak position by $\sim 4kT_{\text{samp}}$. This is justified as the work function is taken as the peak position in the normal direction initially and the positrons inside the solid have thermal kinetic energy. This assumption did not noticeably change the calculated angular distribution. The energy spectra shown in Fig. 6 were calculated using a work function 0.1 eV less than the peak position. It is to be noted that the energy spectra at negative angles show higher energy tailing compared to positive angles and these higher energy positrons might be the cause of the tailing in the angular distribution at negative angles.

At 10° and 16°, the calculated energy spectra start from a slightly lower energy than experimentally observed. In calculating these spectra it was assumed that all positrons in the Maxwellian energy distribution have equal probability for re-emission from the surface. But rather than the actual energy of the positron, it is the component of energy in the direction normal to the surface that would determine its possibility of reaching the surface. Hence, at large angles, higher energy positrons would have a greater probability of reaching the surface though the actual dependence of this probability is difficult to calculate. The assumption of energy-independent probability for reaching the surface could be responsible for the prediction of a greater number of low energy positrons at larger angles than are experimentally observed.

IV. CONCLUSION

Angular distributions and angle-resolved energy distributions of re-emitted positrons in the backward direction have been measured from a W(100) surface at incident energies of 250 and 600 eV and theoretical calculations have been performed in terms of a 1D step model of positron emission. At these low incident energies where implantation depths are small compared to the thermal positron diffusion length, it was necessary to assume an effective sample temperature of four times the actual temperature to reasonably match the observed angular and energy distribution. The increase in the mean energy with deviation from the normal to the surface has been observed in the current measurements. The results qualitatively matched calculations taking into account the energy-dependent refraction of the positrons at the re-emitting surface.

[1]E. M. Gullikson, A. P. Mills, Jr., W. S. Crane, and B. L. Brown, Phys. Rev. B **32**, 5484 (1985).
[2]N. Oshima, R. Suzuki, T. Ohdaira, A. Kinomura, T. Narumi, A. Uedono, and M. Fujinami, Appl. Phys. Lett. **94**, 194104 (2009).
[3]T. Oka, S. Jinno, and M. Fujinami, Anal. Sci. **25**, 837 (2009).
[4]P. J. Schultz and K. G. Lynn, Rev. Mod. Phys. **60**, 701 (1988).
[5]G. Amarendra, K. F. Canter, and D. C. Schoepf, J. Appl. Phys. **80**, 4660 (1996).
[6]R. Suzuki, G. Amarendra, T. Ohadaira, and T. Mikhado, Appl. Surf. Sci. **149**, 66 (1999).
[7]A. Zecca, A. Chiari, A. Sarkar, S. Chattopadhyay, and M. J. Brunger, Nucl. Instrum. Methods Phys. Res., Sect. B **268**, 533 (2010).
[8]N. Oshima, R. Suzuki, T. Ohdaira, A. Kinomura, T. Narumi, A. Uedono, and M. Fujinami, J. Appl. Phys. **103**, 094916 (2008).
[9]M. Kato and A. Ishi, Surf. Sci. **189/190**, 996 (1987).
[10]R. L. Bell, *Negative Electron Affinity Devices* (Clarendon Press, Oxford, 1973).
[11]D. A. Fischer, K. G. Lynn, and D. W. Gidley, Phys. Rev. B **33**, 4479 (1986).
[12]C. A. Murray and A. P. Mills, Jr., Solid State Commun. **34**, 789 (1980).
[13]D. M. Chen, K. G. Lynn, R. Pareja, and B. Nielsen, Phys. Rev. B **31**, 4123 (1985).
[14]Lee Y. Sun, Z. Liu, S. Sun, and P. Pianetta, Appl. Phys. Lett. **91**, 192101 (2007).
[15]H. Zhou, Ph.D. thesis, The University of Texas at Arlington, 1996.
[16]E. Granch, J. Throwe, and K. G. Lynn, Appl. Phys. Lett. **51**, 1862 (1987).
[17]N. Zafar, J. Chevallier, F. M. Jacobsen, M. Charlton, and G. Laricchia, Appl. Phys. **47**, 409 (1988).
[18]F. M. Jacobsen, M. Charlton, J. Chevallier, B. I. Deutch, G. Laricchia, and M. R. Poulsen, J. Appl. Phys. **67**, 575(1990)
[19]B. Jin, O. Sueoka, and A. Hamada, Jpn. J. Appl. Phys. **33**, L1493 (1994).
[20]C. Hugenschmidt, B. Straßer, and K. Schreckenbach, Appl. Surf. Sci. **194**, 283 (2002).
[21]G. Fletcher, J. L. Fry, and P. C. Pattnaik, Phys. Rev. B **27**, 3987 (1983).